

## Pumping based on transverse electrokinetic effects

Irina Gitlin, Abraham D. Stroock, and George M. Whitesides<sup>a)</sup>

*Department of Chemistry and Chemical Biology, Harvard University, Cambridge, Massachusetts 02138*

Armand Ajdari

*Ecole Supérieure de Physique et Chimie Industrielle de Paris, Paris, France*

(Received 12 December 2002; accepted 19 June 2003)

This work presents a strategy for microfluidic pumping based on transverse electro-osmotic flow in a channel with topographical features on one wall. In this channel, flow along the long axis is generated by an electric field applied across the channel. The pump operates at low (5–10 V) voltage and achieves pumping speeds up to  $\sim 100 \mu\text{m/s}$  in submillimeter channels. The pump is straightforward to fabricate, contains no moving parts, and provides local control of the direction and strength of pumping. The performance of the pump scales favorably with decreasing size of a microchannel. © 2003 American Institute of Physics. [DOI: 10.1063/1.1602560]

The microfluidic format—planar chip design, channels with cross-sections of  $\sim 100 \mu\text{m}$ , compatibility with micro-electronic and optical elements—will be widely used in miniaturized devices for chemical and biochemical analysis<sup>1–4</sup> and for high-throughput synthesis.<sup>5</sup> For manipulation of fluid, a functional device must contain components, such as pumps, valves, and mixers, that are durable, easy to fabricate, and easy to activate. The design of microfluidic components should take these characteristics into account.

In this letter, we demonstrate a general strategy for pumping fluids electrically using low voltages ( $\sim 10 \text{ V}$ ). We use a channel that presents obliquely oriented grooves on one wall, and an electric field applied transversely with respect to the principal (long) axis of the channel [Fig. 1(a)]. The applied field drives a primary<sup>6</sup> electro-osmotic flow and pressure-driven recirculation across the channel (along  $e_1$ ). The field and the flow interact with the grooves to generate a net secondary flow along the channel (along  $e_2$ ). We use this secondary flow to pump fluids. We refer to this process as “transverse electro-osmotic flow” (tEOF).

The advantages of pumping by tEOF are that (i) it achieves useful flow speeds ( $\sim 200 \mu\text{m/s}$ ) at low applied voltages and moderate currents ( $\sim 10 \text{ V}$  and  $\sim 50 \mu\text{A}$ , compatible with commercial batteries), because the transverse dimension is small; (ii) pumping magnitude and direction are controlled locally; and (iii) axial dispersion in the patterned region is reduced relative to simple pressure pumping by the mixing in the cross section.<sup>7</sup>

Other methods of pumping in microfluidic systems using electric fields include simple electro-osmosis<sup>8</sup> and electro-osmosis through a packed bed of silica particles.<sup>9</sup> The latter can generate high pressures at low flow rates. Both of these pumping strategies require high voltages ( $> 1000 \text{ V}$ ). Peristaltic pumping—for example, the system developed by Quake and coworkers<sup>10</sup>—provides a practical way to generate and control pressure-driven flow, but requires external gas sources and valves, and is limited to channels in elastomeric material. Pumping schemes based on magnetohydrodynamics have been explored,<sup>11,12</sup> but these techniques cannot be scaled down, since the velocities generated by

magnetic forces scale with the characteristic length of the channel.

The principle of tEOF has been recently described theoretically by Ajdari.<sup>13</sup> It is based on the anisotropic response of the channel with obliquely oriented grooves to an applied field. Consider the general case of a channel of homogeneous surface charge in which shape varies in space (Fig. 1). The principal axes of the channel are  $(e_1, e_2, z)$  and those of the periodic structures on the surface are  $(x, y, z)$  at an angle  $\theta$  with respect to the axes of the channel. In general, the electrokinetic and hydrodynamic response of such a system to applied fields (electric or pressure) is anisotropic: the net flow generated along  $x$  when a field is applied along  $x$  is different than the flow along  $y$  generated by a field of the

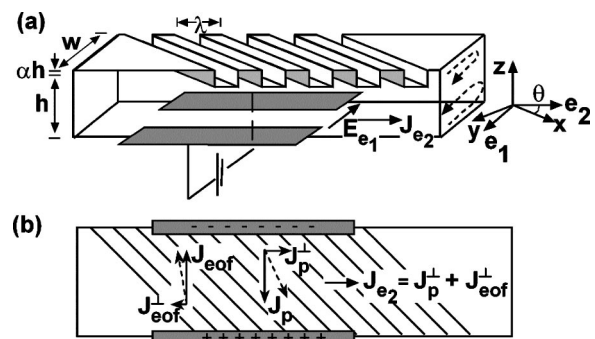


FIG. 1. (a) Schematic diagram of the general channel geometry considered. The principal axes of the walls of the channel are  $(e_1, e_2, z)$ . The principal axes of the surface structures are  $(x, y, z)$  at an angle  $\theta$  to  $(e_1, e_2, z)$ . The principal wavelength of the surface pattern is  $\lambda$ . The average height of the channel is  $h$ . The height varies between  $h + \alpha h$  and  $h - \alpha h$ . The electrodes are shown in gray on the bottom of the channel. Due to the presence of oblique grooves, a transverse electric field  $E_{e_1}$  causes a longitudinal fluid flow  $J_{e_2}$ . In the cross-section is sketched in dashed lines the primary flow pattern which consists of the primary EOF and the consequent pressure-driven recirculation caused by the presence of sidewalls. This pattern is expected to be slightly asymmetric as the electric field, and thus EOF, is larger near the bottom wall containing the electrodes than near the top wall. (b) Top view of the microfluidic channel. Primary electroosmotic flow  $J_{eof}$  (solid vector) generated by the electric field  $E_{e_1}$  causes pressure-driven recirculation  $J_p$  (solid vector). Due to the anisotropic response of the system the primary components of the flow align slightly with the direction parallel to the grooves (dashed vectors). The effect is stronger on the pressure-driven recirculation than on primary EOF; the pressure-driven recirculation governs the direction of the overall net flow generated along the channel.

<sup>a)</sup>Electronic mail: gwhitesides@gmwhgroup.harvard.edu

same strength along  $y$ . In both the pressure-driven and EO flows, the net flow is higher along the grooves (along  $x$ ) than across the grooves (along  $y$ ).

Here, we consider a specific case of an electric field applied along the axis  $e_1$  at an angle  $\theta$  with respect to  $x$  in a channel depicted in Fig. 1. In this geometry, there are two competing terms that contribute to the net longitudinal (along  $e_2$ ) flow:  $\mathbf{J}_{\text{eof}}^\perp$  and  $\mathbf{J}_p^\perp$ , as indicated in Fig. 1(b). The weaker term  $\mathbf{J}_{\text{eof}}^\perp$  arises directly from the interaction of the primary (along  $e_1$ ) EO flow ( $\mathbf{J}_{\text{eof}}$ ) with the grooves. The dominant term  $\mathbf{J}_p^\perp$  is associated with the pressure-driven recirculation of the fluid that is carried across the channel by  $\mathbf{J}_{\text{eof}}$ ;  $\mathbf{J}_p^\perp$  arises from the interaction of this pressure-driven flow with the grooves.<sup>15</sup>

The trajectories of the overall flow are expected to be helical, similar to the ones described by Stroock *et al.*<sup>15,16</sup> and Johnson *et al.*<sup>17</sup> Theoretical treatment of this problem by Ajdari<sup>13</sup> predicts that the amplitude of the net flow induced by perpendicular electric field will be proportional to the applied electric field, to the average surface charge  $\sigma_0$ , and to  $\alpha^2$  for small  $\alpha$ , where  $\alpha$  is the relative height of the grooves to the average height of the channel.

To prepare electrodes, a glass slide was spin-coated and patterned photolithographically with a Shipley 1813 resist in the form of the electrodes. Metals [Cr (4 nm) and Pt (150 nm)] for the electrodes were evaporated onto the patterned slide. The photoresist mask was then lifted off with acetone, leaving the electrodes on the glass slide. To make the channel, a master with positive relief was first prepared using SU8 photoresist in a two-step lithography process.<sup>18</sup> A mold complementary to the master was made in poly(dimethylsiloxane) (PDMS).<sup>19</sup> Fluid reservoirs were cut in PDMS. The PDMS slab was oxidized in a plasma oxidizer, aligned with the electrode pattern, and brought in conformal contact with the slide to define the microfluidic channel [Fig. 1(a)]. The device was used immediately after assembly.<sup>20</sup> We imaged the flow with fluorescent tracer beads of low surface charge (FluoSpheres,<sup>TM</sup> Molecular Probes, 2  $\mu\text{m}$ , polyethylene-glycol (PEG)-modified surface<sup>21</sup>). Prior to each measurement, fresh fluid was flushed through the channel and the fluid level in the reservoirs was carefully balanced to avoid any interference from the residual pressure flow.

We characterized the longitudinal velocities achieved as a function of applied transverse voltage in the channel depicted in Fig. 2(a). Velocities were calculated by measuring the trajectories of the tracer beads over a period of 11 s in the section of the channel clear of pattern. In this section, the flow was simple Poiseuille flow; the velocities represented on the graph in Fig. 2(b) are average velocities over the cross section of the channel.<sup>22</sup> The error bars indicate the extremes in variations in velocities from four sets of experiments. We observed mobilities (defined as velocity per electric field) of 1.1  $\mu\text{m}/(\text{s V}/\text{cm})$  in deionized water and 0.7  $\mu\text{m}/(\text{s V}/\text{cm})$  in 1 mM NaCl solution. The primary EO flow in PDMS channels over glass with smooth walls is  $\sim 6 \mu\text{m}/(\text{s V}/\text{cm})$ .<sup>19</sup> The measured value of the relative magnitude of the secondary flow with respect to the primary flow was  $\sim 1/7$ ; this value is on the order of magnitude predicted by theory.<sup>23</sup>

We demonstrated the operation of the pump in the cases of three- and four-channel junctions. Figures 3(a) and 3(d)

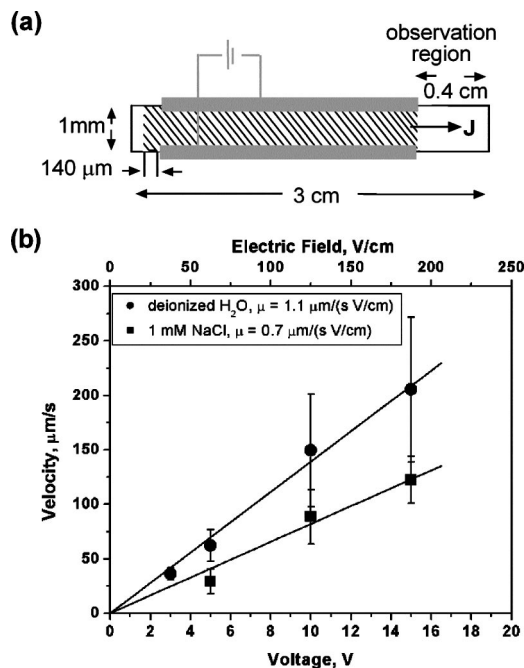


FIG. 2. (a) Top view of a low-voltage pump: The top wall of the channel is patterned with topography; the electrodes in gray are evaporated on the bottom glass surface. The flow is measured in the unpatterned section of the channel clear of electrodes to simplify the visualization. The dimensions of the channel are  $L=3.0$  cm,  $w=1$  mm,  $h=60 \mu\text{m}$ ,  $\alpha=0.16$ ,  $\lambda=140 \mu\text{m}$ . The electrodes are spaced by  $800 \mu\text{m}$ . (b) Velocities plotted as a function of applied transverse electric field. The transverse mobilities  $\mu$  are 1.1  $\mu\text{m}/(\text{s V}/\text{cm})$  in deionized water and 0.7  $\mu\text{m}/(\text{s V}/\text{cm})$  in 1 mM NaCl, found by the linear regression line through the data and the origin.

show the trajectories of the beads at the intersection of the channels as they are pumped with an applied potential of 5 V from two (or three) inlets into one outlet. In the case of four-channel junction [Fig. 3(d)], the trajectories of the beads illustrate hydrodynamic focusing. Figures 3(b), 3(c), 3(e), and 3(f) illustrate the manipulation of the flow with the tEOF pump. The direction of the flow can easily be reversed and directed towards a particular outlet by reversing the polarity of the electrodes [Figs. 3(b), 3(c)]. It is possible to direct the flow through particular branches of the fluidic network by applying voltage in those branches. Disconnecting a voltage source from one or two channels eliminates the tEOF and leaves only pressure-driven flow in those channels. The efficiency with which the flow can be directed through particular branches depends on the passive hydrodynamic resistance along the disconnected channels. The selectivity will thus increase with decreasing size of the channels.

Extended continuous use ( $>3$  min) of the pump is limited by the generation of gas bubbles from the electrolysis of water at the electrodes. Low ionic strength solutions are thus preferable to reduce generation of bubbles<sup>24</sup> and to reduce local  $p\text{H}$  changes at the electrodes.<sup>25</sup> We noticed a drop in velocities of the beads in 1 mM NaCl solutions at applied field of 100 V/cm after 3 min of continuous operation. We attribute this drop to the formation of bubbles on the electrode; these bubbles can be observed using a microscope. The performance of the pump may also be compromised by surface contamination when working with biological samples—a problem inherent in all electro-osmotically driven systems. Surface treatment techniques to minimize

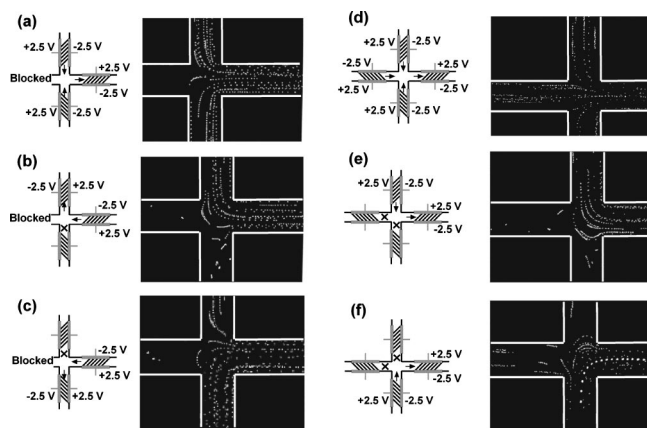


FIG. 3. Demonstration of pumping and local control of the flow by capturing the trajectories of fluorescent beads in systems with three (a)–(c) and four (d)–(f) channels. (a) and (d) show pumping through the channel junctions. (b), (c), (e), and (f) demonstrate reversal of the flow by reversal of the polarity of the electrodes and confinement of the flow to two out of three (or four) channels by disconnecting a channel from the voltage source. The dimensions of the channels are:  $w = 300 \mu\text{m}$ ,  $h = 48 \mu\text{m}$ ,  $\alpha = 0.37$ ,  $\lambda = 140 \mu\text{m}$ . The zone of observation does not include the patterned regions of the channels; the trajectories of the beads are therefore straight. The outlines of the channel walls were enhanced for clarity.

adsorption of proteins and to stabilize EOF, such as the one developed by Linder *et al.*,<sup>26</sup> is applicable to tEOF system as well. A pump with untreated surface may be more compatible with samples of DNA or of small molecules than with protein-rich samples such as cellular extracts.

The pump described in this work produces longitudinal flow electrophoretically in a microchannel, when an electric field is applied across the channel. The pumping effect is caused by the topography on the wall of a microchannel, rather than by an independent pumping unit. It is thus easy to integrate the pumping regions into networks of complex topology, and to control the directions and amplitudes of the flow locally. The voltages necessary to operate the pump are low (e.g., 10 V gives a flow speed of  $\sim 100 \mu\text{m/s}$  in a 1-mm-wide channel), and the pump can be powered by a battery rather than by a high-voltage power supply. This characteristic makes the potential for integration of this pump into a portable microfluidic device attractive. The performance of the tEOF pump improves as the cross-sectional dimensions of the channel are scaled down for several reasons: (i) the required voltage to achieve a given electric field strength (and thus flow speed) is reduced; (ii) the relative strength of the tEOF (the typical velocity is independent of the size of the channel at constant field strength) to pressure-driven flows grows as the typical velocity decreases with size in the latter case; (iii) the generation of gases is reduced as the electrical current through the channel is reduced; and (iv) the diffusion of both heat and dissolved gases out of the channel into the PDMS slab (an effective sink for both heat and gases) occurs more quickly in smaller than in larger channels, so that the tEOF pump can be operated continuously for longer periods of time at higher powers. A disadvantage of this pump is the generation of bubbles when pumping solutions of high ionic strengths ( $> 1 \text{ mM}$ ). We thus recommend this pump for intermittent, rather than continuous, operation (e.g., for injection, sampling, switching, mixing). Alterations

of surface properties of the channel (i.e., the  $\zeta$ -potential) due to adsorption of biological analytes may also jeopardize the performance of this pump.

This work was supported by grants from DARPA and NIH (GM51559). One author (I.G.) thanks NSF for a graduate fellowship. Another (A.A.) thanks the Ministère de la Recherche for support through an ACI Blanche, and acknowledges fruitful discussions with E. Brunet.

- <sup>1</sup>M. A. Burns, C. H. Mastrangelo, T. S. Sammarco, F. P. Man, J. R. Webster, B. N. Johnson, B. Foerster, D. Jones, Y. Fields, A. R. Kaiser, and D. T. Burke, *Proc. Natl. Acad. Sci. U.S.A.* **93**, 5556 (1996).
- <sup>2</sup>A. Y. Fu, C. Spence, A. Scherer, F. H. Arnold, and S. R. Quake, *Nat. Biotechnol.* **17**, 1109 (1999).
- <sup>3</sup>H.-P. Chou, C. Spence, A. Scherer, and S. R. Quake, *Proc. Natl. Acad. Sci. U.S.A.* **96**, 11 (1999).
- <sup>4</sup>S. Takayama, J. C. McDonald, E. Ostuni, M. N. Liang, P. J. A. Kenis, R. I. Ismagilov, and G. M. Whitesides, *Proc. Natl. Acad. Sci. U.S.A.* **96**, 5545 (1999).
- <sup>5</sup>M. C. Mitchell, V. Spikmans, A. Manz, and J. de Mello, *J. Chem. Soc., Perkin Trans. 1* **1**, 514 (2001).
- <sup>6</sup>In this letter, we will always refer to the flow in the direction of the applied electric field as to primary EOF.
- <sup>7</sup>S. W. Jones and W. R. Young, *J. Fluid Mech.* **280**, 149 (1994).
- <sup>8</sup>P. C. H. Li and D. J. Harrison, *Anal. Chem.* **69**, 1564 (1997).
- <sup>9</sup>S. Zeng, C. Chen, J. C. J. Mikkelsen, and J. G. Santiago, *Sens. Actuators B* **79**, 107 (2001).
- <sup>10</sup>M. A. Unger, H.-P. Chou, T. Thorsen, A. Scherer, and S. R. Quake, *Science* **288**, 113 (2000).
- <sup>11</sup>A. V. Lemoff and A. P. Lee, *Sens. Actuators B* **63**, 178 (2000).
- <sup>12</sup>J. Zhong, M. Yi, and H. M. Bau, *Sens. Actuators A* **96**, 59 (2002).
- <sup>13</sup>A. Ajdari, *Phys. Rev. E* **65**, 016301 (2002).
- <sup>14</sup>A more thorough discussion of the relative magnitude of the two effects in the transverse direction will be given elsewhere (E. Brunet, A. Ajdari, in preparation), but the point is clear in the lubrication limit (see Eq. A7 and the coefficients  $M_{21}$  and  $K_{21}$  in Ref. 13).
- <sup>15</sup>A. D. Stroock, S. K. Dertinger, G. M. Whitesides, and A. Ajdari, *Anal. Chem.* **74**, 5306 (2002).
- <sup>16</sup>A. D. Stroock, S. K. W. Dertinger, A. Ajdari, I. Mezic, H. A. Stone, and G. M. Whitesides, *Science* **295**, 647 (2002).
- <sup>17</sup>T. J. Johnson, D. Ross, and L. E. Locascio, *Anal. Chem.* **74**, 45 (2002).
- <sup>18</sup>J. M. K. Ng, I. Gitlin, A. D. Stroock, and G. M. Whitesides, *Electrophoresis* **23**, 3461 (2002).
- <sup>19</sup>D. C. Duffy, J. C. McDonald, O. J. A. Schueller, and G. M. Whitesides, *Anal. Chem.* **70**, 4974 (1998).
- <sup>20</sup>Aged PDMS possesses slightly lower surface mobility than the freshly oxidized PDMS. See Ref. 19 and G. Ocvirik, M. Munroe, T. Tang, R. Oleschuk, K. Westra, and D. J. Harrison, *Electrophoresis* **21**, 107 (2000).
- <sup>21</sup>The reaction of carboxylate functionalized beads (suspension of 2% by weight) with amine-terminated PEG was done in phosphate buffer (200 mM, pH 8) using EDC(30 mg/mL)/NHS(5 mg/ml) coupling. First,  $(\text{EG})_n\text{-NH}_2$  (MW=5000, 200 mg/mL) was allowed to react for 15 min, followed by three consecutive reactions with  $(\text{EG})_3\text{-NH}_2$  (4 mg/mL).
- <sup>22</sup>The system in Fig. 2 consists of a patterned active section of length  $l_p = 2.6 \text{ cm}$  and a passive unpatterned section of length  $l_u = 0.4 \text{ cm}$  assembled in series. The hydrodynamic resistances per unit length of these two sections are similar. We expect the velocities measured in the such system to be smaller by a factor of roughly  $(l_u + l_p)/l_p$  than would be obtained in a fully patterned channel.
- <sup>23</sup>The proportionality constant between the secondary and primary flow rate is  $4\alpha^2 \sin \theta \cos \theta / (1 - 3/4\alpha^2) = 1/8$  for  $\alpha = 1/4$ ,  $\theta = 45^\circ$ .
- <sup>24</sup>We estimate that at 100 V/cm in 1 mM NaCl solution, the average concentration of  $\text{O}_2$  and  $\text{H}_2$  in water at steady state is  $2 \times 10^{-5}$  and  $4 \times 10^{-5} \text{ mol/mL}$ , respectively. These concentrations exceed the solubility limit of these gases in water, and thus can result in formation of bubbles.
- <sup>25</sup>The electrochemical reaction in the absence of electroactive species involves generation of  $\text{H}^+$  ions at the anode [ $2\text{H}_2\text{O} \rightarrow \text{O}_2(\text{g}) + 4\text{H}^+ + 4\text{e}^-$ ] and consumption of  $\text{H}^+$  ions at the cathode [ $2\text{H}^+ + 2\text{e}^- \rightarrow \text{H}_2(\text{g})$ ].
- <sup>26</sup>V. Linder, E. Verpoorte, W. Thormann, N. F. de Rooij, and H. Sigrüst, *Anal. Chem.* **73**, 4181 (2001).